Polyhedral Ruthenaborane Chemistry: Characterization of Several New Ruthenaboranes by Nuclear Magnetic Resonance Spectroscopy, and the Crystal and Molecular Structure of [5,6,6-$(PPh_3)_3$-6-H-*nido*-6-RuB_9H_{12}]*

Norman N. Greenwood, John D. Kennedy, Mark Thornton-Pett, and J. Derek Woollins
Department of Inorganic and Structural Chemistry, University of Leeds, Leeds LS2 9JT

Several new polyhedral ruthenaborane clusters have been synthesized, sometimes in high yield, by the reaction of borane anions with a variety of ruthenium(II) complexes such as $[RuCl_2(PPh_3)_3]$, $[RuH_2(PPh_3)_3]$, $[RuCl_2(PPh_3)_4]$, and $[Ru(CO)ClH(PPh_3)_3]$. Thus *arachno*-$[B_3H_8]^-$ yielded the colourless four-vertex ruthenaborane *arachno*-$[(CO)(PPh_3)_2HRuB_3H_8]$ (**1**), whereas *nido*-$[B_5H_8]^-$ yielded the pale yellow five-vertex cluster *nido*-$[(CO)(PPh_3)_2RuB_4H_8]$ (**2**) and the six-vertex cluster *nido*-$[(CO)(PPh_3)_2RuB_5H_9]$ (**3**). An interesting series of 6-ruthena-*nido*-decaboranes was also synthesized: *arachno*-$[B_9H_{14}]^-$ (and, less effectively, deprotonated *nido*-$B_{10}H_{14}$) yielded orange *nido*-$[(CO)(PPh_3)_2RuB_9H_{13}]$ (**4**) and light yellow *nido*-$[(CO)(PPh_3)_2RuB_9H_{11}(PPh_3)]$ (**5**), whilst *nido*-$[B_9H_{12}]^-$ afforded amber-red crystals of *nido*-$[(PPh_3)_2HRuB_9H_{12}(PPh_3)]$ (**6**). Structures have been assigned on the basis of detailed ^1H, ^{11}B, and ^{31}P n.m.r. studies and comparison with iron, osmium, and iridium analogues where these are known. The structure of [5,6,6-$(PPh_3)_3$-6-H-*nido*-6-RuB_9H_{12}] (**6**) was confirmed by a single-crystal *X*-ray diffraction study; the monoclinic crystals contained $0.25CH_2Cl_2$ as solvent of crystallization [a = 1 263.2(5), b = 1 786.2(3), c = 2 692.8(9) pm, β = 95.09(3)°, U = 6.256 nm^3, space group $P2_1/c$, and Z = 4]. All thirteen H atoms on the cluster were located and freely refined with individual isotropic thermal parameters.

Over the past few years a large number of polyhedral metallaborane cluster compounds have been synthesized and these have been found to exhibit a great variety of structural types.[1-7] Although over 40 metals have now been incorporated as cluster vertices in these compounds there are very few examples of ruthenaboranes. This is particularly surprising in view of (*a*) the extensive chemistry of the ferraboranes,[3,8] (*b*) the known ability of osmium to form stable metallaborane clusters,[9,10] (*c*) the propensity of ruthenium to form hydrocarbon and polyhydride complexes,[11] and (*d*) the prevalence of polynuclear ruthenium carbonyl clusters.[12,13] To date, ruthenaborane chemistry has been limited to the well characterized 'two-vertex' hydrido-bridged BH_4^- complexes,[14] a four-vertex species {mentioned in a review,[15] and which is presumably $[(\eta^5\text{-}C_5H_5)(CO)RuB_3H_8]$ and not $[(\eta^5\text{-}C_5H_5)(CO)_2RuB_3H_8]$ as stated therein}, the *closo*-type five-vertex metal-rich species $[(CO)_{12}Ru_4BH_2]$,[16] and the recent novel *closo*-type compound $[(PPh_3)_2RuB_{10}H_8(OEt)_2]$.[17] In addition, a number of ruthenacarbaboranes have been investigated.[18]

As part of our systematic investigation of the metallaborane chemistry of the heavier metals,[6,19] we now report results of a study of the reactions of some readily available boranes and borane anions (*arachno*-$[B_3H_8]^-$, *nido*-$[B_5H_8]^-$, *nido*-$[B_9H_{12}]^-$, *arachno*-$[B_9H_{14}]^-$, and *nido*-$B_{10}H_{14}$) with the ruthenium(II) complexes $[RuCl_2(PPh_3)_3]$, $[RuH_2(PPh_3)_3]$, $[RuCl_2(PPh_3)_4]$, and $[Ru(CO)ClH(PPh_3)_3]$. These reactions yield a variety of new, air-stable ruthenaboranes and, of these, several four-, five-, six-, and ten-vertex species have been structurally characterized by their n.m.r. spectroscopic similarities to known metallaboranes. In addition, there are several further products which appear to have no parallels in known polyhedral metallaborane chemistry, and which we hope to describe more fully in later papers.[20]

* 6-Hydrido-5,6,6-tris(triphenylphosphine)-*nido*-6-ruthenadecaborane.

Supplementary data available (No. SUP 56300, 6 pp.): thermal parameters, H-atom and solvent co-ordinates. See Instructions for Authors, *J. Chem. Soc., Dalton Trans.*, 1985, Issue 1, pp. xvii—xix. Structure factors are available from the editorial office.

Results and Discussion

(1) *The* arachno-2-*Ruthenatetraborane*, $[(CO)(PPh_3)_2HRuB_3H_8]$ (**1**).—The reaction between $Tl[B_3H_8]$ and $[Ru(CO)ClH(PPh_3)_3]$ in dichloromethane solution at ambient temperature over 20 h gives the colourless, air-stable, crystalline *arachno*-2-ruthenatetraborane $[(CO)(PPh_3)_2HRuB_3H_8]$ (**1**) in 85% yield. This product was readily identified and characterized by analytical data and spectroscopy. The reaction of $[Ru(CO)ClH(PPh_3)_3]$ is analogous to the recently reported osmium reaction[9] which involves metathesis accompanied by the elimination of the two-electron donor PPh_3 [equation (1)].

$$[Ru(CO)ClH(PPh_3)_3] + [B_3H_8]^- \longrightarrow \underset{(1)}{[(CO)(PPh_3)_2HRuB_3H_8]} + Cl^- + PPh_3 \quad (1)$$

The n.m.r. properties of the ruthenatetraborane (**1**) are summarized in Table 1 (see also Table 7) together with those of

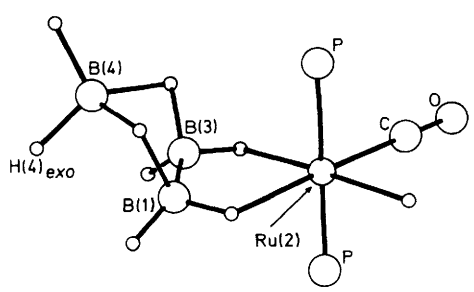

Figure 1. Proposed structure of the four-vertex *arachno*-2-ruthenatetraborane $[(CO)(PPh_3)_2HRuB_3H_8]$ (**1**), with P-phenyl groups omitted

Table 1. Boron-11 and proton n.m.r. data for *arachno*-$[L_3HMB_3H_8]$ (M = Fe, Ru, or Os)

	$[(CO)_3HFeB_3H_8]^a$		$[(CO)(PPh_3)_2HRuB_3H_8]$ (1)^b		$[(CO)(PPh_3)_2HOsB_3H_8]^c$	
Assignment	$\delta(^{11}B)$	$\delta(^1H)$	$\delta(^{11}B)$	$\delta(^1H)$	$\delta(^{11}B)$	$\delta(^1H)$
4	+3.0	+2.95, +2.62	+0.4	+2.60, +1.89	+1.0	+4.34, +2.20
1,3	−42.1	+0.96, +0.68 −0.80, −0.92	−36.7 −38.8	+0.48 −1.33 } −0.51(2 H)^d	−40.5 −39.5	+0.56 −0.83 } −0.21(2 H)^d
H(1,2)		−8.81		−7.23		−9.07
H(2,3)		−12.62		−9.41		−10.20
H_t(M)		−10.66		−9.23^e		−10.10^f

^{a} CD_2Cl_2 solution at ambient temperature; data from ref. 21. ^{b} $CDCl_3$ solution at −36 °C; this work; for ^{31}P data see Table 7. ^{c} $CDCl_3$ solution at 21 °C; data from ref. 9. ^{d} Bridging proton resonances very close together. Note the selective sharpening of $^1H(1,4)$(bridge) and $^1H(3,4)$(bridge) on irradiation at $^{11}B(1)$ and $^{11}B(3)$ only, implying a zero or small coupling $^1J[^{11}B(4)–^1H(bridge)]$. This is typical of *arachno* 4-vertex behaviour in compounds examined so far (see also ref. 9) ^{e} $^2J(^{31}P–^1H_t)$ = 21 Hz. ^{f} $^2J(^{31}P–^1H)$ = 20 Hz.

the osmium analogue[9] and of $[(CO)_3HFeB_3H_8]$.[21] The similarity of the boron-11 and proton n.m.r. chemical shifts of the effective borane ligand in all three compounds confirms the similarity of bonding in the three species as do the results of selective $^1H-\{^{11}B\}$ experiments.[9] As expected, the boron-11 n.m.r. spectrum consists of three distinct boron resonances whereas the proton n.m.r. reveals the presence of eight borane protons, together with a terminal hydride on the ruthenium atom for which the resonance is split into a triplet due to cisoid coupling to two phosphorus-31 nuclei with $^2J(^{31}P–Ru–^1H)$(*cis*) *ca.* 21 Hz. The larger coupling $^2J(^{31}P–Ru–^{31}P)$ of 248 Hz indicates a mutually *trans* disposition of the two phosphorus atoms, with the remaining co-ordination site of the ruthenium being occupied by a carbonyl ligand [$\nu_{max.}$(CO) at 1 975 cm^{-1}]. The proposed geometry is shown in Figure 1.

Of particular interest in the proton n.m.r. investigations was the observation of fluxional behaviour within the effective B_3H_8 ligand unit, involving one of the H(4) protons, the H(1) and H(3) protons, and the two B–H–B protons (for numbering see Figure 1). In the 100-MHz proton spectrum these five protons are equivalent at ≥45 °C but upon cooling to ≤0 °C individual resonances are observed (except for the bridging hydrides which appear accidentally to overlap). This type of fluxionality has been observed previously in the *arachno*-2-manganatetraboranes $[(CO)_4MnB_3H_8]$ and $[(CO)_4MnB_3H_7X]$ (X = Cl, Br, or I)[15] and a mechanism proposed based on the effective rotation of BH_3 units about axes defined approximately by the vectors B(4)–H(4)(*exo*) and B(1)–H(1,2)(bridge). It is of interest that the corresponding osmium compound $[(CO)(PPh_3)_2HOsB_3H_8]$ is static at ambient temperatures,[9] but we have now found that heating does induce analogous fluxionality with proton-resonance coalescence occurring in the 100-MHz spectrum at 70—85 °C. Approximate derived values for $\Delta G^{\ddagger}$ for these processes are *ca.* 55 and *ca.* 65 kJ mol^{-1} respectively for the ruthenium and osmium compounds. The lower activation energy for the ruthenium compound is to be compared to the lower activation energy for the $[(CO)(PPh_3)_2RuB_5H_9]$ decomposition process described below. As far as we are aware, the iron analogues such as $[(CO)_3HFeB_3H_8]$ have not been investigated for fluxionality, although they do appear to be static at ambient temperatures.[15]

(2) *The Five- and Six-vertex* nido-*Ruthenaboranes* $[(CO)(PPh_3)_2RuB_4H_8]$ (**2**) *and* $[(CO)(PPh_3)_2RuB_5H_9]$ (**3**).—Reaction between the *nido*-pentaborane anion $[B_5H_8]^-$ and $[Ru(CO)ClH(PPh_3)_3]$ in thf–CH_2Cl_2 solution at low temperatures gives rise to the pale yellow, air-stable, crystalline five-vertex *nido*-2-ruthenapentaborane [2,2,2-$(CO)(PPh_3)_2$-2-RuB_4H_8] (**2**) in a *ca.* 5% yield, and also [but not yet obtained free of compound (**2**)] the six-vertex *nido*-4-ruthenahexaborane

Table 2. Proton and boron-11 n.m.r. data for *nido*-$[(CO)(PPh_3)_2MB_4H_8]$ [M = Ru (**2**) or Os] in $CDCl_3$ solution at +21 °C^a

	M = Ru (**2**)^b		M = Os^c	
Assignment	$\delta(^{11}B)$	$\delta(^1H)$	$\delta(^{11}B)$	$\delta(^1H)$
4	+8.3	+3.85	+8.9	+6.04
3,5	−9.3 −10.5 } d	+2.68 +1.68 }	−7.5 −14.2	+3.32 +1.41
1	−25.3	+0.66	−34.4	+0.25
B–H–B(bridge)		−1.93 −1.97		−1.68 −2.03
M–H–B(bridge)		−9.31 −9.95^f		−9.75^e −10.34

^{a} *exo*-Terminal ^1H resonances related to directly bound ^{11}B by selective $^1H-\{^{11}B\}$ spectroscopy. ^{b} This work; for ^{31}P data see Table 7. ^{c} Data from ref. 9; note that in ref. 9 some of these values were inadvertently transposed. ^{d} Selective $^1H–^{11}B$ assignments not differentiated by $^1H-\{^{11}B\}$ experiments at 2.34 T. ^{e} Doublet, $^2J(^{31}P–Os–^1H)$ = 37 Hz. ^{f} Doublet, $^2J(^{31}P–Ru–^1H)$ = 47 Hz.

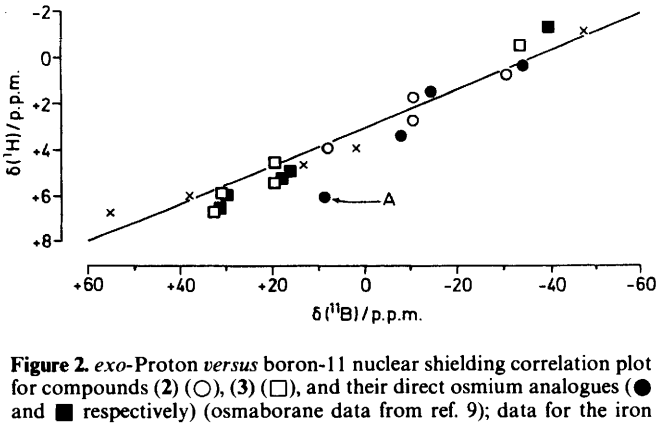

Figure 2. *exo*-Proton *versus* boron-11 nuclear shielding correlation plot for compounds (**2**) (○), (**3**) (□), and their direct osmium analogues (● and ■ respectively) (osmaborane data from ref. 9); data for the iron congener $[(CO)_3FeB_5H_9]$ (×) (ref. 25) are also included. These exhibit reasonable correlation with a line of slope $\delta(^{11}B):\delta(^1H)$ *ca.* 12:1 (compare with Figure 5), the only principal deviation being for the 4-position in the osmium compound $[(CO)(PPh_3)_2OsB_4H_8]$ (datum A) which has a '*trans*' or antipodal distal disposition with respect to the metal centre (*cf.* possibly related '*trans*' effects on ^{11}B shielding: R. Warren, D. Paquin, T. Onak, G. Dunks, and J. R. Spielman, *Inorg. Chem.*, 1970, **9**, 2285)

Table 3. Boron-11 and proton n.m.r. data for $[(CO)(PPh_3)_2RuB_5H_9]$ (**3**), $[(CO)(PPh_3)_2OsB_5H_9]$, and $[(CO)_3FeB_5H_9]$

	$[(CO)(PPh_3)_2RuB_5H_9]$ (3)[a-c]		$[(CO)(PPh_3)_2OsB_5H_9]$[a,b,d]			$[(CO)_3FeB_5H_9]$[f,g]	
Assignment	$\delta(^{11}B)$[h]	$\delta(^1H)$[i]	$\delta(^{11}B)$[h]	$\delta(^1H)$[i]	Assignment[e]	$\delta(^{11}B)$[h,j,k]	$\delta(^1H)$[i,j,l]
3,5	+33.3, +31.5	+6.65, +5.85	+32.2, +30.0	+6.62, +5.85	3,5 3,6	+55.5, +37.7	+6.84, +5.97
2,6	*ca.* +20, *ca.* +19 [m]	+5.42, +4.49	+18.0, +16.4	+5.18, +4.96	2,6 4,5	+13.5, +2.3	+4.53, +3.86
1	−33.4	−0.64	−39.2	−1.49	1 1	−47.0	−1.22
B–H–B		−1.84, −1.96		−2.24, −2.59	B–H–B		+0.82, +0.08, −0.72
M–H–B		−8.53, −9.79[n]		−9.03, −10.59[o]	M–H–B		−16.79

[a] In $CDCl_3$ solution at +21 °C. [b] *exo*-Terminal ^1H resonances related to directly-bonded ^{11}B by selective ^1H-$\{^{11}B\}$ spectroscopy. [c] This work; for ^{31}P data see Table 7. [d] Data from ref. 9. [e] The different bridging H atom disposition for the Fe *versus* the Ru and Os compounds dictates a change in numbering (see footnote * below; note that the absence of one Fe–H–B bridge introduces a 20 p.p.m. disparity in the nuclear shielding of the 3,6 boron atoms. [f] Data from ref. 25. [g] $\delta(^{13}C)$ (*versus* $SiMe_4$) +210.5, +207.7, and +206.6 in $(CD_3)_2CO$ solution at −120 °C. [h] $\delta(^{11}B)$ to low field (high frequency) of $BF_3(OEt_2)$. [i] $\delta(^1H)$ to low field (high frequency) of $SiMe_4$. [j] Compound fluxional at ambient temperatures. [k] In CH_2Cl_2 solution at −80 °C. [l] In $(CD_3)_2CO$ solution at −80 °C. [m] Proximity by ^{11}B resonances precludes differentiation of ^1H assignment by selective ^1H-$\{^{11}B\}$ spectroscopy at 2.34 T. [n] $^2J(^{31}P\text{–}Ru\text{–}^1H)$(*trans*) *ca.* 45 Hz, $^2J(^{31}P\text{–}Ru\text{–}^1H)$(*cis*) *ca.* 12 Hz. [o] $^2J(^{31}P\text{–}Os\text{–}^1H)$(*trans*) = 40 Hz, $^2J(^{31}P\text{–}Os\text{–}^1H)$(*cis*) = 11 Hz.

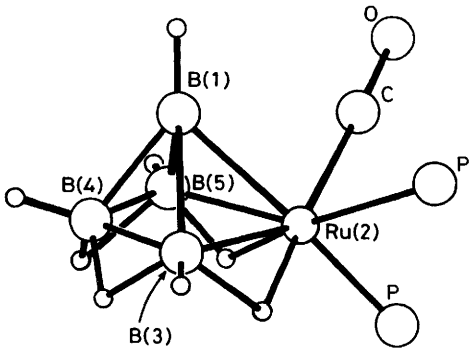

Figure 3. Proposed structure of the five-vertex *nido*-2-ruthenapentaborane $[(CO)(PPh_3)_2RuB_4H_8]$ (**2**), with P-phenyl groups omitted

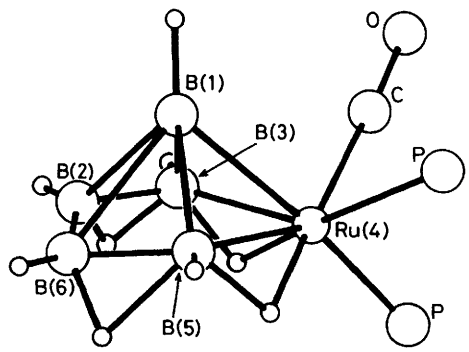

Figure 4. Proposed structure of the six-vertex *nido*-4-ruthenahexaborane $[(CO)(PPh_3)_2RuB_5H_9]$ (**3**), with P-phenyl groups omitted. As with compound (**2**) (Figure 3), n.m.r. spectroscopy establishes the positions of the CO group and one of the PPh_3 groups as transoid to the two bridging B–H–Ru hydrogen atoms

$[4,4,4\text{-}(CO)(PPh_3)_2\text{-}4\text{-}RuB_5H_9]$ (**3**). Phosphorus-31 and boron-11 n.m.r. experiments indicate that, although appreciable quantities of the six-vertex metallahexaborane (**3**) are present in the crude reaction mixture [equation (2)], during work-up or on standing it decomposes to give the five-vertex metallapentaborane (**2**).

$$[Ru(CO)ClH(PPh_3)_3] + [B_5H_8]^- \longrightarrow [(CO)(PPh_3)_2RuB_5H_9] + Cl^- + PPh_3 \quad (2)$$
(**3**)

These observations are consistent with the known conversion of $[4,4,4\text{-}(CO)(PPh_3)_2\text{-}4\text{-}OsB_5H_9]$ to $[2,2,2\text{-}(CO)(PPh_3)_2\text{-}2\text{-}OsB_4H_8]$ in a yield of 40% *via* thermolysis at 100 °C in $CHCl_2CHCl_2$ solution for 1 h;[9] thus the analogous reaction for ruthenium apparently has a lower activation energy (compare the fluxionality of the osma- and ruthena-tetraboranes discussed above). The analogous ferrahexaborane $[2,2,2\text{-}(CO)_3\text{-}2\text{-}FeB_5H_9]$* is also known to decompose to give a ferrapentaborane, but in this decomposition product the iron atom is in the apical 1-position, *i.e.* the compound is $[1,1,1\text{-}(CO)_3\text{-}nido\text{-}1\text{-}FeB_4H_8]$. The corresponding 2-ferrapentaborane $[2,2,2\text{-}(CO)_3\text{-}nido\text{-}2\text{-}FeB_4H_8]$ is also known,[3] but full details have not yet appeared in the literature.

The n.m.r. properties of the five-vertex ruthenapentaborane (**2**) are summarized in Table 2 and Figure 2 (see also Table 7), together with those[9] for the direct osmium analogue $[(CO)(PPh_3)_2OsB_4H_8]$. The structure is readily established from the n.m.r. data, with the four distinct boron-11 resonances indicating that the ligands on the metal centre are arranged asymmetrically with respect to the metallaborane cluster. The proton n.m.r. spectrum shows (apart from four terminal B–H resonances) two B–H–B and two M–H–B resonances, with one of the latter exhibiting splitting arising from coupling to phosphorus-31 of $^2J(^{31}P\text{–}Ru\text{–}^1H)$ = 47 Hz, *i.e.* in the range typical for bridging hydride and phosphorus atoms in a mutually *trans* disposition.[9,22-25] The i.r. spectrum is also consistent with the above data as well as revealing the presence of a Ru-co-ordinated carbonyl ligand [$\nu_{max.}$(CO) at 1 940

* The numbering of the six-vertex *nido*-metallaboranes is the I.U.P.A.C. recommended one based on that of the neutral *nido*-hexaborane B_6H_{10}. In this, the basal unbridged position is bounded by B(2) and B(6), so that the iron atom in $[(CO)_3FeB_5H_9]$, which is flanked by an unbridged basal linkage, takes the 2-descriptor, whereas the ruthenium and osmium atoms in $[(CO)(PPh_3)_2RuB_5H_9]$ and $[(CO)(PPh_3)_2OsB_5H_9]$, which are opposite the unbridged site, take the 4-descriptor.

cm^{-1}]. The above together with microanalytical data (see Table 7) establishes the constitution and geometry of the molecule (Figure 3).

The species can be conveniently regarded as consisting of a tridentate *arachno*-$[B_4H_8]^{2-}$ ligand which co-ordinates to the three vacant orbitals of the d^6 ruthenium(II) centre $[Ru(CO)(PPh_3)_2]^{2+}$; in these terms the ruthenium centre contributes a vertex but no additional bonding electrons to the cluster and this effects the notional transition from four-vertex *arachno* to five-vertex *nido*. The transition-metal centre has an 18-electron configuration. In cluster terms the neutral $Ru(CO)(PPh_3)_2$ fragment is equivalent to a neutral BH group, contributing three orbitals and two electrons to the cluster bonding scheme; it is thus very similar to the well established cluster behaviour of the analogous $Fe(CO)_3$ grouping.[3,8]

As mentioned above [equation (2)] the reaction between *nido*-$[B_5H_8]^-$ and $[Ru(CO)ClH(PPh_3)_3]$ also yields significant quantities of what we believe to be the six-vertex *nido*-metallahexaborane $[(CO)(PPh_3)_2RuB_5H_9]$ (**3**). We have not yet been able to obtain this compound free of the five-vertex homologue (**2**), and the formulation of its structure relies on the comparison of its n.m.r. properties (Table 3 and Figure 2; see also Table 7) with those of the analogous osmium complex.[9] However, the striking similarities of these properties clearly establish the compound as exactly analogous to $[(CO)(PPh_3)_2OsB_5H_9]$, both compounds being *nido*-metallahexaboranes with the metal atom occupying the basal position equivalent to B(4) in the parent hexaborane B_6H_{10} (see Figure 4).

The electronic structure of compound (**3**) may be interpreted in a similar manner to (**2**) as an 18-electron d^6 ruthenium(II) complex, now with an effective tridentate *arachno*-$[B_5H_9]^{2-}$ ligand. In these terms, similarly, the ruthenium centre $[Ru(CO)(PPh_3)_2]^{2+}$ adds an additional vertex but no additional bonding electrons to the 16-electron borane cluster, thus effecting the notional *arachno* five-vertex to *nido* six-vertex transition. It is of interest that in both the ruthenium and osmium complexes the B(2)–B(6) position distal from the metal centre is the one which lacks the hydrogen bridge, whereas in the iron analogue $[(CO)_3FeB_5H_9]$ it is the proximal Fe(2)–B(6) position * that is unbridged;[26] furthermore, in the anionic iron species $[(CO)_3FeB_5H_8]^-$, both the Fe(2)–B(3) and B(3)–B(4) positions are unbridged, and the distal B(4)–B(5) position still remains bridged.[27] In this context it is worth noting than in smaller metal–boron and metal–carbon clusters containing iron or osmium there is often a marked preference for bridging hydrogen atoms to favour osmium and to avoid iron.[3,7]

In contrast to most metallahexaboranes which have fewer than five basal-bridging hydrogen atoms,[7,26–29] including B_6H_{10} itself,[30] the ruthenium and osmium compounds reported here are not fluxional with respect to basal-bridging hydrogen-atom site exchange.

(3) *The Ten-vertex* nido-6-*Ruthenadecaboranes* $[(CO)(PPh_3)_2RuB_9H_{13}]$ (**4**), $[(CO)(PPh_3)_2RuB_9H_{11}(PPh_3)]$ (**5**), *and* $[(PPh_3)_2HRuB_9H_{12}(PPh_3)]$ (**6**).—The reaction of $[Ru(CO)ClH(PPh_3)_3]$ with $[NEt_4][B_9H_{14}]$ in CH_2Cl_2 solution at ambient temperature for 2 d gives the *nido* ten-vertex species $[(CO)(PPh_3)_2RuB_9H_{13}]$ (**4**) as an orange crystalline solid (yield 35%) [equation (3)], together with smaller quantities of a second *nido* ten-vertex compound $[(CO)(PPh_3)_2RuB_9H_{11}(PPh_3)]$ (**5**) as a light yellow crystalline solid (*ca.* 5% yield). Compounds (**4**) and (**5**) are also obtained (but in much smaller yields) from the reaction of $[Ru(CO)H_2(PPh_3)_3]$ with either $[NEt_4][B_9H_{14}]$ or $[B_{10}H_{12}]^{2-}$ (assumed to be formed *in situ*, or in incipient form, from $B_{10}H_{14}$ and two equivalents of *NNN'N'*-tetramethylnaphthalene-1,8-diamine during the reaction process). Other products from these reactions include the phosphine boranes $B_9H_{13}(PPh_3)$ and $BH_3(PPh_3)$. Characterization of (**4**) and (**5**) as *nido*-6-ruthenadecaboranes was readily accomplished by microanalysis (Table 7) and n.m.r. spectroscopy (Tables 4 and 7).

$$[Ru(CO)ClH(PPh_3)_3] + [B_9H_{14}]^- \longrightarrow [(CO)(PPh_3)_2RuB_9H_{13}] + H_2 + Cl^- + PPh_3 \quad (3)$$
(**4**)

The similarity of the nuclear shielding and coupling data of the ruthenaborane (**4**) (Table 4 and Figure 5) with those of the

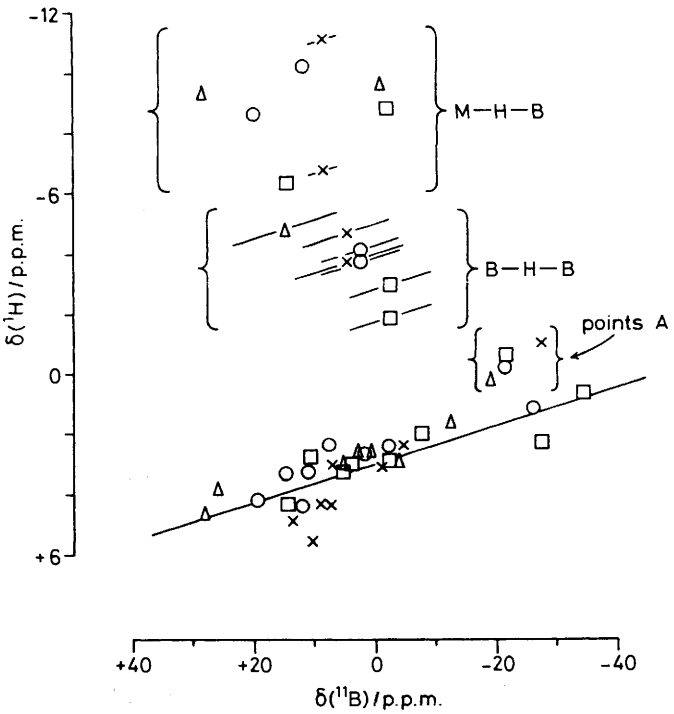

Figure 5. Proton *versus* boron-11 nuclear shielding correlation plot for the ten-vertex *nido*-6-ruthenadecaborane species $[(CO)(PPh_3)_2RuB_9H_{13}]$ (**4**) (○), $[(CO)(PPh_3)_2RuB_9H_{11}(PPh_3)]$ (**5**) (△), $[(PPh_3)_2HRuB_9H_{12}(PPh_3)]$ (**6**) (□), and the iridium analogue $[(PPh_3)_2HIrB_9H_{13}]$ (×, data from ref. 22). The line drawn has slope $\delta(^{11}B):\delta(^1H)$ of 16:1 (compare with Figure 2 and refs. 39—44). The $\delta(^1H)$ higher shielding deviation of the data for the 2-positions (data A) has also been noted for other *nido*-6-metalladecaboranes (refs. 24 and 39) and may be diagnostic of this structural type. The B–H–B bridging protons at 4—10 p.p.m. above the line and the M–H–B bridging ones at 10—15 p.p.m. above the line are also in diagnostically typical ranges

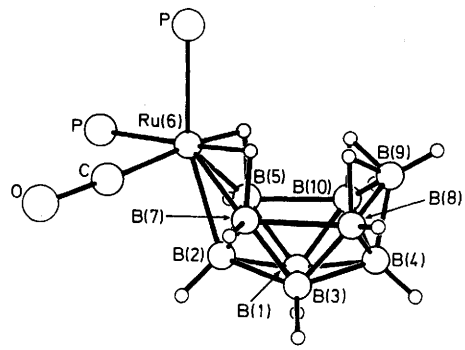

Figure 6. Proposed structure of $[(CO)(PPh_3)_2RuB_9H_{13}]$ (**4**) with P-phenyl groups omitted

* See footnote on previous page.

Table 4. Proton and boron-11 n.m.r. data[a] for $[(CO)(PPh_3)_2RuB_9H_{13}]$ (**4**), $[(CO)(PPh_3)_2RuB_9H_{11}(PPh_3)]$ (**5**), $[(PPh_3)_2HRuB_9H_{12}(PPh_3)]$ (**6**), and $[(PPh_3)_2HIrB_9H_{13}]$

Tentative assignment	Compound (**4**)[b]		Compound (**5**)[c]		Compound (**6**)[b]		$[(PPh_3)_2HIrB_9H_{13}]$[c,d]	
	$\delta(^{11}B)$[e]	$\delta(^1H)$[f]	$\delta(^{11}B)$[e]	$\delta(^1H)$[f]	$\delta(^{11}B)$[e]	$\delta(^1H)$[f]	$\delta(^{11}B)$[e]	$\delta(^1H)$[f]
9	+7.4[g]	+2.47	*ca.* +3[h]	+2.76	+5.4[g,h]	+3.28	+13.2	+4.94
1,3	+14.7[i]	+3.36	+5.6	+2.92	+10.7[i]	+2.88	+9.0	+4.39
	+11.2[i]	+3.35	+0.4	+2.71	+3.4[i]	+2.93	+7.5	+4.33
5,7	+11.9[g,j]	+4.49	+28.0[k]	+4.69	+14.6[g,l]	+4.37	+10.5	+5.64
	+19.8[g,m]	+4.27	−4.0[n]	+2.99	−2.4[g,o]		+6.5	+3.14
8,10	+1.7[g]	+2.73	−8.9[h]		−1.8[g,h]	+2.98	−1.0	+3.05
	−2.1[g]	+2.49	+26.0[h]	+3.82	−7.7[g,h]	+2.08	−4.8	+2.37
2,4	−21.6[i,p]	−0.15[p]	−12.5[q]	+1.70[q]	−21.5[i,p]	−0.51[p]	−27.5[q]	+2.37[q]
	−26.1[i,q]	+1.17[q]	−19.4[p]	+0.27[p]	−34.4[i,q]	+0.72[q]	−27.8[p]	−0.99[p]
B–H–B		−3.92		−4.76		−2.80		−3.77
		−4.09				−3.99		−4.58
M–H–B		−8.56[m]		−9.26[k]		−6.26[l,r]		−6.64[t]
		−10.23[j]		−9.52[n]		−8.73[o,r,s]		−11.08[u]

[a] For ^{31}P data see Table 7. [b] In CD_2Cl_2 solution at +21 °C. [c] In $CDCl_3$ solution at +21 °C. [d] From ref. 22. [e] $\delta(^{11}B)$ ±0.5 p.p.m. to high frequency (low field) of $BF_3(OEt_2)$. [f] $\delta(^1H)$ ±0.05 p.p.m. to high frequency (low field) of $SiMe_4$; *exo*-terminal ^1H resonances related to directly-bound ^{11}B positions by selective ^1H-$\{^{11}B\}$ experiments; $^1J(^{11}B–^1H)(exo)$ where measurable is in the range 140—160 Hz. [g] Broader resonance; resonances for $^{11}B(6,9)$ and $^{11}B(5,7,8,10)$ are generally broader in *nido*-decaborane analogues, which aids assignment (see also footnote *i*). [h] Assignments among 8,9,10 positions tentative (see text). [i] Sharper resonance; resonances for $^{11}B(2,4)$ and $^{11}B(1,3)$ are generally the sharper in *nido*-decaborane analogues, which aids assignment (see also footnote *g*). [j] $\delta(^1H)$ −10.23, doublet, $^2J(^{31}P–Ru–^1H)$ = 44 Hz, selectively sharpened by $\nu(^{11}B)$ corresponding to $\delta(^{11}B)$ *ca.* +12; this assigns $\delta(^1H)$ −10.23 *trans* to PPh_3 and $\delta(^{11}B)$ +11.9 to B(7). [k] $\delta(^1H)$ −9.26, doublet, $^2J(^{31}P–Ru–^1H)$ = 60 Hz; this is selectively sharpened by $\nu(^{11}B)$ corresponding to $\delta(^{11}B)$ +28.0 which therefore assigns $\delta(^1H)$ −9.26 *trans* to PPh_3 and $\delta(^{11}B)$ +28.0 to B(5). [l] 7-Position; selective sharpening of $\delta(^1H)$ −6.26 on irradiation at $\nu(^{11}B)$ corresponding to $\delta(^{11}B)$ +14.6. [m] $\delta(^1H)$ −8.56 selectively sharpened to a singlet by irradiation at $\nu(^{11}B)$ = corresponding to $\delta(^{11}B)$ +19.8; this assigns $\delta(^1H)$ −8.56 *trans* to CO and $\delta(^{11}B)$ +19.8 to B(5). [n] $\delta(^1H)$ −9.52 selectively sharpened to a singlet by $\nu(^{11}B)$ corresponding to $\delta(^{11}B)$ −4.0 which assigns $\delta(^1H)$ −9.52 *trans* to CO and $\delta(^{11}B)$ −4.0 to B(7). [o] Phosphine-bound B(5) position; $^1J(^{31}P–^{11}B)$ = 128 Hz; also $^1J[^{11}B–^1H(bridge)]$ *ca.* 60 Hz between $\delta(^{11}B)$ −2.4 and $\delta(^1H)$ −8.73. [p] Probably 2-position [see ref. 39; the tentative assignments of BH(2) and BH(4) in ref. 22 have now been reversed]. [q] Probably 4-position (see ref. 39). [r] Also Ru–^{1}H(terminal) at $\delta(^1H)$ −11.03 with $^2J(^{31}P–Ru–^1H)(cis)$ = 23.5 and 24.5, $^3J(^{31}P–B–Ru–^1H)$ = 14.7, and possible $^2J(^1H–Ru–^1H)(trans)$ 2.3 Hz. [s] Exhibits $^2J(^{31}P–Ru–^1H)(trans)$ = 18.3 Hz and fine structure due to other couplings $^nJ(^1H–^1H)$ and $^nJ(^{31}P–^1H)$. [t] Exhibits coupling $^2J(^1H–Ir–^1H)(trans)$ 6.5 Hz to Ir–^{1}H(terminal) at $\delta(^1H)$ −12.30; this last also has $^2J(^{31}P–Ir–^1H)(cis)$ = 18 and 19 Hz. [u] Doublet $^2J(^{31}P–Ir–^1H)(trans)$ = 66 Hz.

well characterized[22] *nido*-iridadecaborane [6,6,6-$(PPh_3)_2$H-6-IrB_9H_{13}] enables compound (**4**) to be identified without difficulty as a direct structural analogue, *viz.* [6,6,6-$(CO)(PPh_3)_2$-*nido*-6-RuB_9H_{13}] (Figure 6).

For compound (**4**), boron-11 and proton n.m.r. spectroscopy indicate nine inequivalent boron atoms, each with one terminal hydrogen atom bound to it. Also apparent are two B–H–B together with two M–H–B bridging hydrogen-atom proton resonances, one of the latter being split into a doublet, with $^2J(^{31}P–Ru–^1H)$ = 44 Hz, as a result of *trans* coupling to a phosphine. These signals were assigned and related by ^1H-$\{^{11}B\}$ selective-decoupling n.m.r. experiments. Phosphorus-31 n.m.r. spectroscopy (Table 7) shows the presence of two mutually *cis* phosphine ligands on the metal, with $^2J(^{31}P–Ru–^{31}P)(cis)$ = 24 Hz, whilst the i.r. spectrum shows the presence of a metal-bound carbonyl group [$\nu_{max.}$(CO) at 1 995 cm^{-1}]. The structure of compound (**4**) is thus reasonably shown to be that in Figure 6.

The previously reported ten-vertex iridium analogue $[(PPh_3)_2HIrB_9H_{13}]$[22] is related to compound (**4**) by the notional interchange of a neutral $Ru(CO)(PPh_3)_2$ moiety with an isoelectronic $IrH(PPh_3)_2$ grouping; both of these fragments provide two electrons and three orbitals for the *nido* ten-vertex cluster bonding, in an analogous manner to the neutral BH fragment in the 6-position of the parent *nido*-decaborane, $B_{10}H_{14}$, itself. Both metal centres can be regarded as 18-electron d^6 centres with a quasi-octahedral six-bonding-orbital geometry as in the ruthenapentaborane and ruthenahexaborane compounds (**2**) and (**3**) discussed above (Figure 3 and 4).

N.m.r. spectroscopy (summarized in Table 4 and Figure 5, see also Table 7) shows that the second ruthenadecaborane (**5**) has a closely related structure, formulated as [6-(CO)-(6,6,8 or 10)-$(PPh_3)_3$-*nido*-6-RuB_9H_{11}] (Figure 7). The nine inequivalent *nido*-6-metalladecaboranyl boron atoms are readily apparent, but selective ^1H-$\{^{11}B\}$ experiments show the presence of only 11 cluster hydrogen atoms, and that one of the boron atoms does not have a terminal hydrogen atom. Proton resonances for two M–H–B bridging hydrogen atoms are apparent [of which one exhibits coupling $^2J(^{31}P–Ru–^1H)(trans)$ of *ca.* 60 Hz], but only one B–H–B proton resonance is present. Phosphorus-31 n.m.r. at lower temperatures[31,32] shows the presence of two sharp doublets, with $^2J(^{31}P–Ru–^{31}P)$ = 22 Hz, together with a broader resonance at higher field (Table 7). The former can be assigned to two mutually *cis* phosphine ligands on the ruthenium centre, whilst the latter is assigned to a PPh_3 grouping attached in an *exo*-terminal position to a boron atom. The presence of a carbonyl ligand on the metal atom [$\nu_{max.}$(CO) at 1 980 cm^{-1}] is readily evident from i.r. spectroscopy, and the $Ru(CO)(PPh_3)_2$ metal environment in compound (**5**) is thus analogous to that in $[(CO)(PPh_3)_2RuB_9H_{13}]$ (**4**). The absence of a bridging hydrogen atom to the point of subrogation is a common characteristic when H_2BH(bridge) units are (notionally) replaced by isoelectronic BPR_3 or CH centres,[25] which thus reasonably locates the third phosphine substituent position as B(8) [or B(10)] or B(9) on the borane cluster. Of these two possibilities, the grosser deviations from symmetry in the boron-11 n.m.r. spectrum over that observed in compound (**1**), together with the differential ^1H-$\{^{11}B\}$ decoupling effects on the B–H–B bridging proton when the $^{11}B(8)$, $^{11}B(9)$, and $^{11}B(10)$ resonance positions are selectively irradiated, reasonably discount the possibility of the phosphine substituent being at the 9-position. The compound therefore has this third phosphine substituent on B(8) or B(10), but in the absence of *X*-ray crystallographic data it is not possible to distinguish whether this substituent position is *syn* [*i.e.* at position B(8) as shown in Figure 7] or *anti* [position B(10), not shown] to the carbonyl group on the ruthenium centre. Other possible

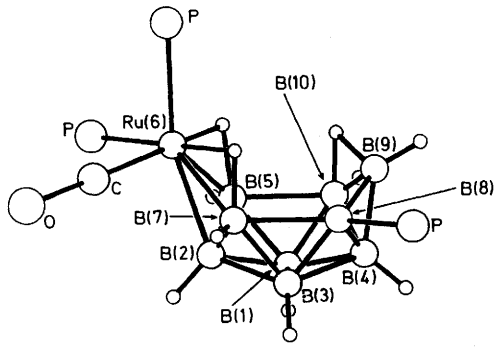

Figure 7. Proposed structure of $[(CO)(PPh_3)_2RuB_9H_{11}(PPh_3)]$ (**5**) with P-phenyl groups omitted. As drawn it has the boron-bound PPh_3 grouping in the 8-position cisoid to the carbonyl ligand on the metal atom. Present evidence cannot distinguish between this and the transoid 10-position (see text)

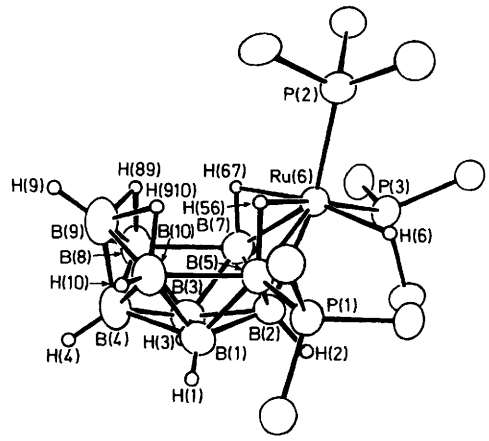

Figure 8. A drawing of the crystallographically determined molecular structure of $[(PPh_3)_2HRuB_9H_{12}(PPh_3)]$ (**6**) showing the metallaborane cluster and phosphine ligands with *ipso*-carbon atoms only

structures in principle would include a 5-ruthenadecaborane species but the presence of two M–H–B bridging hydrogen atoms discounts this structure.

Definitive assignments of individual resonances in the boron-11 and proton spectra of compound (**5**) do of course have to remain tentative at present, with the exception of the signals arising from the 5- and 7-positions which are established from selective ^1H-$\{^{11}B\}$ double-resonance experiments and the presence of couplings $^2J(^{31}P\text{–}Ru\text{–}^1H)$ to the phosphine ligands on the metal.

Electronically, both *nido*-6-ruthenadecaborane compounds (**4**) and (**5**) can be described as *nido* ten-vertex species, with the metal vertex providing two electrons and three orbitals for cluster bonding to result in d^6 ruthenium(II) compounds which have a quasi-octahedral bonding orbital geometry as also occurs in the smaller clusters of the five- and six-vertex ruthenaborane compounds (**2**) and (**3**) discussed above.

A third related compound, $[5,6,6\text{-}(PPh_3)_3\text{-}6\text{-}H\text{-}nido\text{-}6\text{-}RuB_9H_{12}]$ (**6**), is formed in small yield as an air-stable, amber-red, crystalline solid in the reaction between $[RuCl_2(PPh_3)_4]$ and $[NBu^n_4][B_9H_{12}]$ in dichloromethane solution. In this case we have been able to characterize the compound structurally, by a single-crystal *X*-ray diffraction analysis, as an example of this structural type. All atoms were located, including Ru–H(6)-(terminal), and an ORTEP drawing of the metallaborane cluster is given in Figure 8. Selected interatomic distances are given in Table 5, and angles between interatomic vectors in Table 6.

Table 5. Selected interatomic distances (pm) for $[5,6,6\text{-}(PPh_3)_3\text{-}6\text{-}H\text{-}nido\text{-}6\text{-}RuB_9H_{12}]$ (**6**) with estimated standard deviations in parentheses

(*i*) From the ruthenium atom

Ru(6)–B(2)	230.0(10)	Ru(6)–H(6)	185.1(84)
Ru(6)–B(5)	231.1(10)	Ru(6)–H(5,6)	197.4(63)
Ru(6)–B(7)	226.3(11)	Ru(6)–H(6,7)	195.2(87)
Ru(6)–P(2)	232.3(4)	Ru(6)–P(3)	231.1(4)

(*ii*) Boron–boron

B(1)–B(2)	175.5(14)	B(3)–B(2)	178.4(14)
B(1)–B(3)	176.4(15)		
B(1)–B(4)	176.8(14)	B(3)–B(4)	179.0(16)
B(1)–B(5)	178.6(14)	B(3)–B(7)	177.1(15)
B(1)–B(10)	176.8(15)	B(3)–B(8)	172.2(15)
B(2)–B(5)	179.1(14)	B(2)–B(7)	182.5(15)
B(4)–B(10)	181.6(16)	B(4)–B(8)	175.1(17)
B(4)–B(9)	172.0(18)		
B(5)–B(10)	201.1(22)	B(7)–B(8)	205.8(20)
B(9)–B(10)	181.0(15)	B(8)–B(9)	178.6(17)

(*iii*) Boron–hydrogen

B(1)–H(1)	83(7)	B(3)–H(3)	81(8)
B(2)–H(2)	113(7)	B(4)–H(4)	109(8)
B(7)–H(7)	96(7)		
B(8)–H(8)	112(9)	B(10)–H(10)	111(7)
B(9)–H(9)	112(8)		
B(5)–H(5,6)	139(6)	B(7)–H(6,7)	125(9)
B(8)–H(8,9)	148(9)	B(10)–H(9,10)	130(9)
B(9)–H(8,9)	114(9)	B(9)–H(9,10)	145(7)

(*iv*) Phosphorus–carbon and phosphorus–boron

P(1)–C(111)	182.3(6)	P(2)–C(211)	187.4(7)	P(3)–C(311)	186.6(6)
P(1)–C(121)	182.5(6)	P(2)–C(221)	187.4(7)	P(3)–C(321)	187.7(6)
P(1)–C(131)	183.9(6)	P(2)–C(231)	186.9(6)	P(3)–C(331)	187.5(6)

B(5)–P(1) 197.8(10)

(*v*) Other

Phenyl rings were constrained to C–C 139.5 pm, C–H 108 pm, H–C–C 120° and C–C–C 120°.

The structure is that of a *nido*-6-metallaborane, the *nido*-decaboranyl nature of the cluster being readily apparent from the location of the bridging hydrogen atoms in the (5,6)(6,7) and (8,9)(9,10) positions, and in the longer distances B(5)–B(10) and B(7)–B(8) of 201.1(22) and 205.8(20) pm respectively (*cf.* 197 pm in $B_{10}H_{14}$ itself[33]). The boron cage phosphine substituent is at the 5-position, and the retention of the bridging hydrogen atoms indicates that the structure may be regarded as notionally derived from an effective tridentate *arachno*-type $[B_9H_{12}\text{-}(PPh_3)]^-$ ligand co-ordinated to the cationic ruthenium(II) d^6 centre $[RuH(PPh_3)_2]^+$.

In terms of the neutral cluster-fragment approach, the compound is again an 18-electron transition-metal complex with the neutral $RuH(PPh_3)_2$ group contributing three orbitals, but now only one electron, to the cluster bonding within the quasi-octahedral metal bonding orbital geometry. The other three metal co-ordination sites are occupied by the two phosphines and the hydride ligand. Taken with the straightforward metallaborane species (**4**) described above, it represents an interesting effective neutral ligand ⟷ hydride ion interchange of two-electron donors between a site on the metal centre and a site on the borane cluster. It is of interest that this notional interchange of a charged site with a neutral one does not markedly perturb the electronic structure as judged by n.m.r. shielding parameters. This has also been noted for a variety of iridaborane cluster compounds[25,34] and other related

Table 6. Selected angles (°) between interatomic vectors for [5,6,6-$(PPh_3)_3$-6-H-*nido*-6-RuB_9H_{12}] (**6**) with estimated standard deviations in parentheses

(*i*) At ruthenium atom

P(2)–Ru(6)–P(3)	100.3(2)	P(3)–Ru(6)–H(6)	86(3)
P(2)–Ru(6)–H(6)	89(3)	P(3)–Ru(6)–H(5,6)	170(2)
P(2)–Ru(6)–H(5,6)	82(2)	P(3)–Ru(6)–H(6,7)	94(3)
P(2)–Ru(6)–H(6,7)	101(3)	P(3)–Ru(6)–B(2)	96.9(3)
P(2)–Ru(6)–B(2)	163.7(1)	P(3)–Ru(6)–B(5)	137.8(2)
P(2)–Ru(6)–B(5)	118.1(3)	P(3)–Ru(6)–B(7)	85.8(3)
P(2)–Ru(6)–B(7)	134.1(2)		
H(6)–Ru(6)–H(5,6)	84(3)	B(2)–Ru(6)–H(5,6)	81(2)
H(6)–Ru(6)–H(6,7)	170(4)	B(2)–Ru(6)–H(6,7)	78(3)
H(6)–Ru(6)–B(2)	92(3)	B(2)–Ru(6)–B(5)	45.7(3)
H(6)–Ru(6)–B(5)	78(3)	B(2)–Ru(6)–B(7)	47.1(3)
H(6)–Ru(6)–B(7)	137(3)		
H(5,6)–Ru(6)–H(6,7)	95(3)	H(6,7)–Ru(6)–B(5)	95(3)
H(5,6)–Ru(6)–B(5)	37(2)	H(6,7)–Ru(6)–B(7)	34(3)
H(5,6)–Ru(6)–B(7)	100(2)	B(5)–Ru(6)–B(7)	80.0(4)

(*ii*) Ruthenium–boron–boron

Ru(6)–B(2)–B(1)	121.4(6)	Ru(6)–B(2)–B(3)	118.4(6)
Ru(6)–B(2)–B(5)	67.5(5)	Ru(6)–B(2)–B(7)	65.4(5)
Ru(6)–B(5)–B(1)	119.3(6)	Ru(6)–B(7)–B(3)	120.9(6)
Ru(6)–B(5)–B(2)	66.8(5)	Ru(6)–B(7)–B(2)	67.5(5)
Ru(6)–B(5)–B(10)	124.2(6)	Ru(6)–B(7)–B(8)	121.9(5)

(*iii*) Selected other angles

B(5)–B(2)–B(7)	108.3(7)	B(5)–P(1)–C(111)	114.9(4)
B(8)–B(4)–B(10)	106.2(7)	B(5)–P(1)–C(121)	112.9(4)
Ru(6)–P(2)–C(211)	122.9(3)	B(5)–P(1)–C(131)	113.4(4)
Ru(6)–P(2)–C(221)	108.4(3)	P(1)–B(5)–B(1)	110.4(6)
Ru(6)–P(2)–C(231)	120.4(3)	P(1)–B(5)–B(2)	124.2(6)
Ru(6)–P(3)–C(311)	118.4(3)	P(1)–B(5)–B(10)	108.4(6)
Ru(6)–P(3)–C(321)	111.7(3)	P(1)–B(5)–Ru(6)	121.5(5)
Ru(6)–P(3)–C(331)	120.4(3)	P(1)–B(5)–H(5,6)	101(3)

species.[20,35] It does not however hold when the electronic structure is somewhat more modified; for example the replacement of a terminal hydrogen plus a bridging hydrogen atom by *one exo*-terminal phosphine produces much more marked changes in the cluster shielding patterns [*e.g.* compound (**5**), Table 4].

Compared with the cage-phosphine substituted species (**5**) described above, the notional addition of a further hydrogen atom to a cluster bridging position would produce an extra electron for cluster bonding; this is removed by substitution, on the metal atom, of the two-electron donor CO group on (**5**) by the one-electron donor H atom in (**6**), thus retaining the ten-vertex *nido* electron count.

The proton, boron-11, and phosphorus-31 n.m.r. properties (Table 4 and Figures 4 and 9; see also Table 7) are consistent with the structure, and tentative assignments can be made as indicated in the tabulation. Points of interest include the coupling of the phosphorus-31 nucleus of the boron-bound phosphine ligand to adjacent nuclei. That to the directly bound B(5) nucleus, $^1J(^{31}P–^{11}B)$ of *ca.* 130 Hz, is within normal ranges,[32] but the coupling $^2J(^{31}P–Ru–^1H)$ to the M–H–B bridging proton is effectively zero ($\leqslant$ *ca.* 3 Hz), whereas the corresponding coupling $^1J[^{11}B(5)–^1H(bridge)]$ seems to be quite large for a bridging proton coupling at *ca.* 60 Hz. There is also a vicinal cisoid coupling $^3J(^{31}P–B–Ru–^1H)$ of *ca.* 15 Hz to the ruthenium-bound terminal hydrogen. A number of instances of this last type of coupling have recently been reported in polyhedral metallaborane-type species, for example

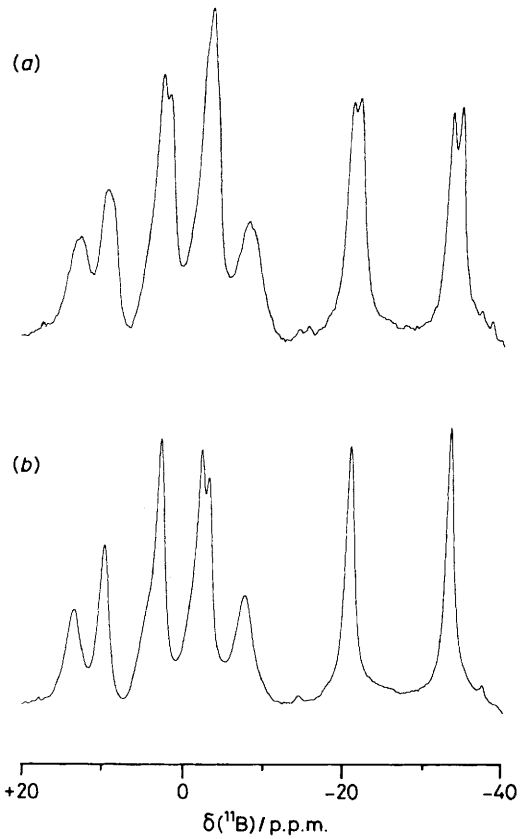

Figure 9. 115-MHz (*a*) ^{11}B and (*b*) ^{11}B-{^1H(broad-band noise)} n.m.r. spectra of [$(PPh_3)_2HRuB_9H_{12}(PPh_3)$] (**6**)

$^3J(^{31}P–Ir–B–^1H)$ of *ca.* 31 Hz in [$(PMe_3)_3HIrB_8H_{12}$][36] and *ca.* 33 Hz in [$(CO)_3(PPh_3)(o\text{-}Ph_2PC_6H_4)_2Ir_2B_4H_2$];[34,37] and $^3J(^{31}P–B–Ir–^1H)$ of *ca.* 25 Hz in [1,2,2-$(PPh_3)_3$-2-H-*closo*-2,10-$IrCB_8H_8$][38] and *ca.* 8 Hz in [$(PMe_2Ph)_2ClHReB_9H_{12}$(P-$Me_2Ph$)].[39] It is not observed in all instances of this geometry, however; for example in [$(CO)(PMe_3)_2IrB_8H_{11}$][23] no coupling is observed for an ostensibly similar cisoid vicinal disposition, indicating that there is also a strong dependence on the intermediate boron–metal cluster bonding, which is not unexpected. These three-bond (and also longer range) couplings between nuclei of atoms bonded *exo* to the cluster are becoming increasingly well documented in polyhedral boron compounds, and are of increasing diagnostic value. Other recent examples in ten-vertex borane cluster chemistry include an examination of $^2J(^1H–B–^1H)$ and $^3J(^1H–B–B–^1H)$ and related couplings in *nido*-decaboranyl systems,[40] and the observation of both cisoid and transoid couplings $^5J(^{31}P–M–B–B–M–^{31}P)$ (M = Ni, Pd, Pt, or Ir) of up to *ca.* 15 Hz in *arachno*-dimetalladecaborane species.[23,35,41,42]

Experimental

General and Spectroscopy.—Unless stated otherwise initial reactions were carried out under nitrogen or using standard vacuum techniques; subsequent manipulations were carried out in air. Preparative thin-layer chromatography (t.l.c.) was performed using 20 × 20 × 0.1 cm plates (Kieselgel 60G, Merck) which were made in the laboratory as required. The compounds [$RuCl_2(PPh_3)_3$], [$RuH_2(PPh_3)_3$], [$RuCl_2(PPh_3)_4$], [$Ru(CO)ClH(PPh_3)_3$], Tl[*arachno*-B_3H_8], [NBu^n_4][*nido*-B_9H_{12}], and [NEt_4][*arachno*-B_9H_{14}] were prepared by standard methods.

Table 7. Microanalytical, ^{31}P n.m.r., and $\nu(CO)_{max.}$ data for compounds (**1**)—(**6**)

Compound	Analysis (%)[a] C	H	B	P	$\delta(^{31}P)$/ p.p.m.[b]	$^2J(^{31}P-Ru-^{31}P)$/ Hz	Conditions for ^{31}P n.m.r.	$\nu(CO)_{max.}$/ cm^{-1}
(**1**)	63.8	5.85	4.3	9.0	+43.9	248[c]	−35 °C, $CDCl_3$	1 975
	(63.3)	(5.7)	(4.75)	(9.1)	+48.7			
(**2**)		5.95	5.9		+48.5	21[d]	−50 °C, $CDCl_3$	1 940
		(5.4)	(6.15)		+34.2			
(**3**)	*e*	*e*	*e*	*e*	+45.6	24[d]	−50 °C, $CDCl_3$	*e*
					+36.4			
(**4**)		5.8	12.2	7.75	+45.6	24[d]	−35 °C, CH_2Cl_2–CD_2Cl_2	1 995
		(5.65)	(12.7)	(8.1)	+43.4			
(**5**)			9.0	9.7	+47.4	22[d]	−40 °C, CD_2Cl_2	1 980
			(9.5)	(9.1)	+41.9			
					+12.8[f]			
(**6**)[g]					+65.3	34[d]	−50 °C, $CDCl_3$	
					+59.7			
					+14.2[f]			

[a] Calculated values in parentheses. [b] $\delta(^{31}P)$ to high frequency (low field) of 85% H_3PO_4. [c] *trans* Coupling. [d] *cis* Coupling. [e] Not obtained free of (**2**) (see text). [f] Broad resonance, the broadness arising from partially collapsed coupling $^1J(^{31}P-^{11}B)$. [g] Insufficient quantities for elemental analysis.

Proton (100 MHz) and phosphorus-31 (40 MHz) n.m.r. spectra were obtained on a 2.34 T JEOL FX-100 spectrometer in these laboratories; double- and triple-resonance $^1H-\{^{11}B\}$ and $^1H-\{^{11}B,^1H\}$ experiments were carried out as described elsewhere.[22,40,43,44]

Phosphorus-31 n.m.r. was generally performed at lower temperatures (*ca.* −50 °C) to maximize the 'thermal decoupling' of boron-10 and boron-11 nuclei from the phosphine ligand resonances.[31] Boron-11 spectra at 128 MHz were recorded using a Bruker WH-400 instrument (S.E.R.C. Service, University of Sheffield), and 115.5-MHz boron-11 and 360-MHz proton spectra [in $^1H-\{^{11}B$(selective)$\}$ experiments] on a Bruker WH-360 instrument (S.E.R.C. Service, University of Edinburgh). Chemical shifts $\delta(^{31}P)$ and $\delta(^{11}B)$ are given in p.p.m. to high frequency (low field) of 85% H_3PO_4 (Ξ 40 480 730 Hz) and $BF_3(OEt_2)$–$CDCl_3$ (Ξ 32 083 971 Hz)[32] respectively. Infrared spectra were recorded on a Pye Unicam SP 2000 spectrophotometer with the samples prepared as pressed KBr discs.

Preparation of $[(CO)(PPh_3)_2HRuB_3H_8]$ (**1**).—$Tl[B_3H_8]$ (0.244 g, 1 mmol) and $[Ru(CO)ClH(PPh_3)_3]$ (0.47 g, 0.5 mmol) were stirred together in CH_2Cl_2 (25 cm^3) at room temperature for 20 h. After filtration the solution was reduced in volume to *ca.* 2 cm^3 and applied to preparative t.l.c. plates. Elution using CH_2Cl_2–light petroleum (b.p. 60—80 °C) (4:1) gave $BH_3(PPh_3)$ (R_f 0.95) and the title compound (**1**) (R_f 0.7) as a colourless solid which was recrystallized from CH_2Cl_2, with addition of pentane, to give 0.305 g (0.42 mmol, 85%) of the product. Analytical and n.m.r. data are given in Tables 1 and 7.

Preparation of $[(CO)(PPh_3)_2RuB_4H_8]$ (**2**) and $[(CO)(PPh_3)_2RuB_5H_9]$ (**3**).—Tetrahydrofuran (20 cm^3) was condensed into a two-necked 250-cm^3 flask containing LiMe (0.4 cm^3 of 2.5 mol dm^{-3} diethyl ether solution, 1 mmol). One arm of the flask carried a tipper tube containing $[Ru(CO)ClH(PPh_3)_3]$ (0.47 g, 0.5 mmol) whilst the other was connected to the vacuum line. The flask was cooled to −197 °C and B_5H_9 (1 mmol) condensed in. The flask was then allowed to warm to −78 °C. After 20 min, CH_2Cl_2 (50 cm^3) was condensed in at −78 °C and the ruthenium complex added. The mixture was stirred and allowed to warm up to room temperature slowly (4—5 h) to give a clear yellow solution. This was reduced in volume (rotary evaporator) and chromatographed using CH_2Cl_2–light petroleum (1:1) to give the light yellow title complex (**2**) (R_f 0.95) and also $[(CO)(PPh_3)_2RuB_5H_9]$ (**3**) (R_f 0.8), which, as discussed in the text, has not yet been isolated in a pure state because of its ready decay to give compound (**2**) at room temperature. The yields of (**2**) and (**3**) were *ca.* 5 and *ca.* 1% respectively. Analytical data are in Table 7, and the n.m.r. properties are summarized in Tables 2 and 3. The compounds were characterized as described in the text. Traces of $[(CO)(PPh_3)_2HRuB_3H_8]$ (**1**) and $BH_3(PPh_3)$ were also detected in the reaction mixture.

Preparation of $[(CO)(PPh_3)_2RuB_9H_{13}]$ (**4**), *and of* $[(CO)(PPh_3)_2RuB_9H_{11}(PPh_3)]$ (**5**).—$[NEt_4][B_9H_{14}]$ (0.24 g, 1 mmol) and $[Ru(CO)ClH(PPh_3)_3]$ (0.47 g, 0.5 mmol) were stirred together in CH_2Cl_2 (50 cm^3) at room temperature for 2 d. The resulting orange-brown solution was chromatographed twice using CH_2Cl_2–light petroleum (b.p. 60—80 °C) (1:1) as eluant to yield compounds (**4**) (R_f 0.8) and (**5**) (R_f 0.7). These were recrystallized by addition of light petroleum to solutions in dichloromethane to give compound (**4**) as a bright orange solid (130 mg, 35%) and compound (**5**) as a light yellow solid (30 mg, 5%). Analytical data are given in Table 7, and the n.m.r. parameters summarized in Tables 4 and 5. The compounds were characterized as described in the text.

Preparation of $[(PPh_3)_2HRuB_9H_{12}(PPh_3)]$ (**6**).—A procedure using $[RuCl_2(PPh_3)_3]$ as the starting material is described. A similar procedure using $[RuCl_2(PPh_3)_4]$ gave very similar results. A solution of $[RuCl_2(PPh_3)_3]$ (1.44 g, 1.5 mmol) and $[NBu^n_4][B_9H_{12}]$ (0.52 g, 1.5 mmol) in CH_2Cl_2 (60 cm^3) was stirred at room temperature for 20 h. The solution darkened during this time. The resulting mixture was filtered through silica gel, and the filtrate reduced in volume (rotary evaporator). Preparative t.l.c. [CH_2Cl_2–light petroleum (b.p. 60—80 °C) (1:4) as eluant] yielded a number of components in small quantities together with somewhat larger amounts of an amber-red component with R_f 0.7. This last component was purified by repeated chromatography (column and t.l.c.), using mixtures of light petroleum (b.p. 60—80 °C) and CH_2Cl_2 as eluants; this gave compound (**6**) as a burgundy-red solid. A final purification by t.l.c. using diethyl ether as eluant, followed by recrystallisation effected by slow diffusion of diethyl ether into a solution in CH_2Cl_2, yielded crystals suitable for *X*-ray diffraction analysis. Insufficient quantities have so far been obtained in pure form for definitive elemental analysis, but the identity readily follows

Table 8. Atom co-ordinates ($\times 10^4$) for the non-hydrogen atoms of [5,6,6-$(PPh_3)_3$-6-H-*nido*-6-RuB_9H_{12}] (**6**)

Atom	*x*	*y*	*z*	Atom	*x*	*y*	*z*
Ru(6)	8 068	5 800	3 329	C(215)	4 896(3)	7 067(3)	4 687(2)
B(1)	9 615(7)	6 475(5)	2 388(4)	C(216)	5 870(3)	6 720(3)	4 639(2)
B(2)	8 795(6)	5 755(5)	2 576(3)	C(221)	8 467(4)	6 984(2)	4 323(2)
B(3)	10 193(7)	5 610(5)	2 577(4)	C(222)	9 552(4)	6 898(2)	4 279(2)
B(4)	10 948(7)	6 457(6)	2 650(4)	C(223)	10 255(4)	7 477(2)	4 423(2)
B(5)	8 589(6)	6 694(4)	2 780(3)	C(224)	9 873(4)	8 141(2)	4 613(2)
B(7)	9 539(7)	5 242(5)	3 079(3)	C(225)	8 788(4)	8 227(2)	4 658(2)
B(8)	10 987(7)	5 777(6)	3 119(4)	C(226)	8 085(4)	7 649(2)	4 513(2)
B(9)	11 040(7)	6 754(6)	3 260(4)	C(231)	7 651(4)	5 552(2)	4 641(1)
B(10)	10 034(7)	7 174(6)	2 827(4)	C(232)	8 576(4)	5 497(2)	4 962(1)
P(1)	7 557(1)	7 398(1)	2 439(1)	C(233)	8 638(4)	4 975(2)	5 349(1)
C(111)	6 187(2)	7 067(2)	2 371(2)	C(234)	7 776(4)	4 509(2)	5 415(1)
C(112)	5 965(2)	6 352(2)	2 181(2)	C(235)	6 851(4)	4 564(2)	5 093(1)
C(113)	4 915(2)	6 107(2)	2 102(2)	C(326)	6 788(4)	5 086(2)	4 706(1)
C(114)	4 086(2)	6 576(2)	2 213(2)	P(3)	7 322(1)	4 618(1)	3 290(1)
C(115)	4 308(2)	7 292(2)	2 403(2)	C(311)	5 977(3)	4 491(3)	3 514(2)
C(116)	5 358(2)	7 537(2)	2 482(2)	C(312)	5 261(3)	5 085(3)	3 457(2)
C(121)	7 509(4)	8 297(2)	2 759(2)	C(313)	4 248(3)	5 015(3)	3 621(2)
C(122)	7 114(4)	8 920(2)	2 491(2)	C(314)	3 953(3)	4 349(3)	3 842(2)
C(123)	7 096(4)	9 617(2)	2 723(2)	C(315)	4 669(3)	3 754(3)	3 899(2)
C(124)	7 472(4)	9 691(2)	3 224(2)	C(316)	5 681(3)	3 825(3)	3 735(2)
C(125)	7 868(4)	9 068(2)	3 492(2)	C(321)	7 071(3)	4 282(3)	2 632(1)
C(126)	7 886(4)	8 370(2)	3 259(2)	C(322)	6 056(3)	4 350(3)	2 385(1)
C(131)	7 859(4)	7 638(3)	1 803(1)	C(323)	5 880(3)	4 155(3)	1 883(1)
C(132)	8 600(4)	8 200(3)	1 735(1)	C(324)	6 719(3)	3 891(3)	1 628(1)
C(133)	8 866(4)	8 373(3)	1 256(1)	C(325)	7 733(3)	3 823(3)	1 874(1)
C(134)	8 392(4)	7 985(3)	846(1)	C(326)	7 909(3)	4 018(3)	2 376(1)
C(135)	7 650(4)	7 423(3)	913(1)	C(331)	8 050(4)	3 805(2)	3 601(2)
C(136)	7 384(4)	7 250(3)	1 392(1)	C(332)	8 069(4)	3 091(2)	3 392(2)
P(2)	7 565(1)	6 201(1)	4 094(1)	C(333)	8 490(4)	2 491(2)	3 677(2)
C(211)	6 244(3)	6 644(3)	4 169(2)	C(334)	8 892(4)	2 606(2)	4 170(2)
C(212)	5 644(3)	6 916(3)	3 748(2)	C(335)	8 873(4)	3 320(2)	4 379(2)
C(213)	4 669(3)	7 264(3)	3 796(2)	C(336)	8 451(4)	3 919(2)	4 094(2)
C(214)	4 295(3)	7 339(3)	4 266(2)				

from the results of *X*-ray crystallography (see below, Tables 5 and 6, and Figure 8), and n.m.r. spectroscopy (Tables 4 and 7) as discussed in the text.

X-*Ray Study of* [$(PPh_3)_2HRuB_9H_{12}(PPh_3)$] (**6**).—Intensity data were collected on a Syntex $P2_1$ diffractometer, operating in the ω—2θ scan mode using graphite-monochromatized Mo-K_α radiation (λ = 71.069 pm), and following a procedure described elsewhere in detail.[45] The structure was solved and refined *via* standard heavy-atom procedures and full-matrix least squares (in two blocks) using the SHELX program system.[46] All non-hydrogen atoms (excluding a CH_2Cl_2 solvent molecule, refined with a 0.25 occupancy factor and an overall thermal parameter) were assigned anisotropic thermal parameters. All phenyl groups were included in the refinement as rigid bodies with hexagonal symmetry (C–C = 139.5 pm). All phenyl hydrogen atoms were included in calculated positions (C–H = 108 pm) and refined with an overall isotropic thermal parameter for each group. All other hydrogen atoms were located experimentally and refined freely with individual isotropic thermal parameters. The weighting scheme $\omega = 1/[\sigma^2(F_o) + g(F_o)^2]$ was applied in which the parameter *g* was included in the refinement to give a flat analysis of variance with increasing sinθ and $(F/F_{max.})^{\frac{1}{2}}$. Atomic co-ordinates are given in Table 8.

Crystal data. $C_{54}H_{58}B_9P_3Ru{\cdot}0.25CH_2Cl_2$, M = 1 019.64, monoclinic, a = 1 263.2(5), b = 1 786.2(3), c = 2 692.8(9) pm, β = 95.09(3)°, U = 6.256 nm^3, space group $P2_1/c$, Z = 4, D_c = 1.08 g cm^{-3}, μ = 5.50 cm^{-1}, $F(000)$ = 2 220.

Data collection parameters. Scans running from 1° below $K_{\alpha 1}$ to 1° above $K_{\alpha 2}$, scan speeds 2.0—29.3° min^{-1}, $4.0 < 2\theta < 45.0°$. 8 281 Unique data, 6 028 observed [$I > 2\sigma(I)$], T = 290 K.

Structure refinement. Number of parameters = 578, weighting factor g = 0.000 69, R = 0.0588, R' = 0.0604.

Acknowledgements

We thank the S.E.R.C. for support, Dr. David Reed (Edinburgh University) for services in high-field n.m.r. spectroscopy, Dr. Jonathan Bould for discussions and some experimental assistance, Johnson Matthey for the loan of some ruthenium complexes, and Alan Hedley for microanalyses.

References

1 N. N. Greenwood and I. M. Ward, *Chem. Soc. Rev.*, 1974, **3**, 231.
2 R. N. Grimes (ed.), 'Metal Interactions with Boron Clusters,' Plenum Press, London and New York, 1982.
3 C. E. Housecroft and T. P. Fehlner, *Adv. Organomet. Chem.*, 1982, **21**, 57.
4 R. N. Grimes, in 'Comprehensive Orgamometallic Chemistry,' eds. G. Wilkinson, F. G. A. Stone, and E. W. Abel, Pergamon, Oxford, 1982, vol. 1, ch. 5.5, p. 459.
5 K. B. Gilbert, S. K. Boocock, and S. G. Shore, in 'Comprehensive Organometallic Chemistry,' eds. G. Wilkinson, F. G. A. Stone, and E. W. Abel, Pergamon, Oxford, 1982, vol. 6, ch. 14.1, p. 879.
6 N. N. Greenwood, *Pure Appl. Chem.*, 1983, **55**, 1415.
7 J. D. Kennedy, *Prog. Inorg. Chem.*, 1984, **32**, 519; and in the press.
8 N. N. Greenwood and J. D. Kennedy, in 'Metal Interactions with Boron Clusters,' ed. R. N. Grimes, Plenum Press, London and New York, 1982, ch. 2, p. 43.

9 J. Bould, N. N. Greenwood, and J. D. Kennedy, *J. Organomet. Chem.*, 1983, **249**, 11.
10 J. Bould, J. E. Crook, N. N. Greenwood, and J. D. Kennedy, *J. Chem. Soc., Chem. Commun.*, 1983, 951.
11 M. A. Bennett, M. I. Bruce, and T. W. Matheson, in 'Comprehensive Organometallic Chemistry,' eds. G. Wilkinson, F. G. A. Stone, and E. W. Abel, Pergamon, Oxford, 1982, vol. 4, ch. 32.3, p. 691; ch. 32.4, p. 821.
12 M. I. Bruce, in 'Comprehensive Organometallic Chemistry,' eds. G. Wilkinson, F. G. A. Stone, and E. W. Abel, Pergamon, Oxford, 1982, ch. 32.5, p. 843; ch. 32.6, p. 889.
13 P. R. Raithby, in 'Transition Metal Clusters,' ed. B. F. G. Johnson, Wiley, New York, 1980, ch. 2, p. 7.
14 J. B. Letts, T. J. Mazanec, and D. W. Meek, *J. Am. Chem. Soc.*, 1982, **104**, 3898 and refs. therein.
15 D. F. Gaines and S. J. Hildebrandt, in 'Metal Interactions with Boron Clusters,' ed. R. N. Grimes, Plenum Press, London and New York, 1982, ch. 3, p. 119.
16 C. R. Eady, B. F. G. Johnson, and J. Lewis, *J. Chem. Soc., Dalton Trans.*, 1977, 477.
17 J. E. Crook, M. Elrington, N. N. Greenwood, J. D. Kennedy, and J. D. Woollins, *Polyhedron*, 1984, **3**, 901.
18 E. H. S. Wong and M. F. Hawthorne, *Inorg. Chem.*, 1978, **17**, 2863.
19 N. N. Greenwood, *Pure Appl. Chem.*, 1983, **55**, 77; see also, N. N. Greenwood, in 'Inorganic Chemistry: Toward the 21st Century,' ed. M. H. Chisholm, *ACS Symp. Ser.*, 1983, **211**, ch. 22, p. 333; N. N. Greenwood, in 'Rings, Clusters, and Polymers of the Main Group Elements,' ed. A. H. Cowley, *ACS Symp. Ser.*, 1983, **232**, ch. 8., p. 125.
20 See, for example, J. E. Crook, M. Elrington, N. N. Greenwood, J. D. Kennedy, M. Thornton-Pett, and J. D. Woollins, following paper.
21 D. F. Gaines and S. J. Hildebrandt, *Inorg. Chem.*, 1978, **17**, 794.
22 S. K. Boocock, J. Bould, N. N. Greenwood, J. D. Kennedy, and W. S. McDonald, *J. Chem. Soc., Dalton Trans.*, 1982, 713.
23 J. Bould, N. N. Greenwood, and J. D. Kennedy, *J. Chem. Soc., Dalton Trans.*, 1984, 2477.
24 M. A. Beckett, N. N. Greenwood, J. D. Kennedy, and M. Thornton-Pett, *J. Chem. Soc., Dalton Trans.*, in the press.
25 J. Bould, Ph.D. Thesis, University of Leeds, 1983.
26 S. G. Shore, J. D. Ragaini, R. L. Smith, C. E. Cottrell, and T. P. Fehlner, *Inorg. Chem.*, 1979, **18**, 670.
27 T. P. Fehlner, J. Ragaini, M. Mangion, and S. G. Shore, *J. Am. Chem. Soc.*, 1976, **98**, 7085.
28 R. Wilczynski and L. G. Sneddon, *Inorg. Chem.*, 1979, **18**, 864.
29 N. N. Greenwood, J. D. Kennedy, W. S. McDonald, D. Reed, and J. Staves, *J. Chem. Soc., Dalton Trans.*, 1979, 117.
30 V. T. Brice, H. D. Johnson, and S. G. Shore, *J. Am. Chem. Soc.*, 1973, **95**, 6629.
31 J. D. Kennedy and J. Staves, *Z. Naturforsch., Teil B.*, 1979, **34**, 808.
32 J. D. Kennedy, in 'Multinuclear N.M.R. (N.M.R. in Inorganic and Organometallic Chemistry),' ed. J. Mason, Plenum, London and New York, in the press.
33 A. Tippe and W. C. Hamilton, *Inorg. Chem.*, 1969, **8**, 1464.
34 J. E. Crook, Ph.D. Thesis, University of Leeds, 1982.
35 M. A. Beckett, Y. M. Cheek, N. N. Greenwood, and J. D. Kennedy, unpublished work.
36 J. Bould, J. E. Crook, N. N. Greenwood, and J. D. Kennedy, *J. Chem. Soc., Dalton Trans.*, 1984, 1903.
37 J. E. Crook, N. N. Greenwood, J. D. Kennedy, and W. S. McDonald, *J. Chem. Soc., Chem. Commun.*, 1982, 383.
38 N. W. Alcock, J. G. Taylor, and M. G. H. Wallbridge, *J. Chem. Soc., Chem. Commun.*, 1983, 1168.
39 M. A. Beckett, J. D. Kennedy, N. N. Greenwood, and M. Thornton-Pett, *J. Chem. Soc., Dalton Trans.*, 1985, 1119.
40 M. A. Beckett and J. D. Kennedy, Abstracts NATO N.M.R. Advanced Study Institute, Stirling, 1982.
41 S. K. Boocock, N. N. Greenwood, M. J. Hails, J. D. Kennedy, and W. S. McDonald, *J. Chem. Soc., Dalton Trans.*, 1981, 1415.
42 N. N. Greenwood, M. J. Hails, J. D. Kennedy, and W. S. McDonald, *J. Chem. Soc., Dalton Trans.*, 1985, 953.
43 J. D. Kennedy and N. N. Greenwood, *Inorg. Chim. Acta*, 1980, **38**, 93.
44 J. D. Kennedy and B. Wrackmeyer, *J. Magn. Reson.*, 1980, **38**, 529.
45 A. Modinos and P. Woodward, *J. Chem. Soc., Dalton Trans.*, 1974, 2065.
46 G. M. Sheldrick, SHELX 76, 'Program System for *X*-Ray Structure Determination,' University of Cambridge, 1976.

Received 5*th February* 1985; *Paper* 5/207